16th World Conference on Earthquake, 16WCEE 2017
Santiago Chile, January 9th to 13th 2017
Paper N° 1500 (Abstract ID)
Registration Code: S- Q1461053754

HIGHLY EFFICIENET SEMI-ACTIVE OIL DAMPER FOR STRUCTURAL CONTROL WITH ENERGY RECOVERY SYSTEM

R. Fukuda[(1)], H. Kurino[(2)]

[(1)] Chief Engineer, Architectural Design Division, Kajima Corp.,fukudar@kajima.com
[(2)] Senior Group Leader, Architectural Design Division, Kajima Corp.,kurino@kajima.com

Abstract

This paper presents a novel semi-active oil damper developed to break through the limitations of existing oil dampers by introducing a unique energy recovery system. The proposed device is equipped with an auxiliary oil tank outside the main cylinder, and oil flows between the cylinder and the tank are controlled by solenoid valves. Existing oil dampers change vibration energy to heat. However, the proposed device recovers the vibration energy as strain energy of oil in the tank and reuses it at an optimum timing to improve the control efficiency. Its mechanical model is expressed as a four-element model that consists of a Maxwell model and a Voigt model in series. First, we present the basic configuration of the device, and show how the energy recovery system works in accordance with the control algorithm. Second, we show the results of dynamic loading tests conducted on a full-scale specimen and the results of simulation analyses using the four-element model. Finally, we demonstrate the results of seismic response analyses using a high-rise building model, and discuss the control effect in comparison with existing oil dampers.

Keywords: Energy recovery, Semi-active control, oil damper, dynamic loading test

1. Introduction

Among various types of damping devices for structural control, the oil damper is a typical example of a high-performance device. It can absorb large vibration energy of buildings caused by earthquakes, and can also control small-amplitude vibrations caused by wind forces. In 2000, we developed a variable oil damper that was able to increase energy absorption efficiency under the constraint of the Maxwell model by controlling the damping coefficient based on an on/off control algorithm [1]. This variable oil damper has been installed in more than 30 high-rise buildings in 15 years in Japan, and its excellent performance beyond that of conventional linear viscous oil dampers has been verified through vibration tests or observation records [2]. However, it is true that demand for a more efficient control device has increased as a result of experiences in the Great East Japan Earthquake of 2011. In that earthquake, lots of high-rise buildings in metropolitan areas continued shaking with large amplitude and long duration. Although there was no severe structural damage, residents were very uneasy and became concerned about the sense of security against earthquakes. Consequently, a highly effective control device that reduces not only maximum amplitudes but also the duration of vibrations has become required.

This paper presents a novel semi-active oil damper developed to break through the limitations of existing oil dampers by introducing a unique energy recovery system. The proposed device is equipped with an auxiliary oil tank outside the main cylinder, and the oil flows between the cylinder and the tank are controlled by solenoid valves. Existing oil dampers, including variable types, always change the vibration energy to heat. However, the proposed device recovers the vibration energy as strain energy of oil in the auxiliary tank and reuses it at an optimum timing to improve control efficiency. Its mechanical model is expressed as a four-element model that consists of a Maxwell model and a Voigt model in series. The spring element of the additional Voigt model, which represents the energy recovery system, plays an important role. First, we present the basic configuration of the device, and show how the energy recovery system works in accordance with the control algorithm. The

control efficiency is also discussed quantitatively based on the four-element model. Second, we show the results of dynamic loading tests conducted on a full-scale specimen and the results of simulation analyses using the four-element model. Finally, we demonstrate the results of seismic response analyses using a high-rise building model, and discuss the control effect in comparison with existing oil dampers.

2. Review of existing oil dampers

In this section, we review the energy absorption capacity of existing oil dampers, which is important for comparison with the proposed damper. Fig.1 shows the basic configuration of the variable oil damper developed by the authors [1, 3]. The control valve in the damper placed between the hydraulic chambers and valve openings can be changed. The conventional linear viscous oil damper has the same configuration as the variable damper, but the valve V_C is adjusted to give it linear characteristics. A simplified mechanical model of these dampers installed in a structure by connecting them with a brace or a wall is expressed as a Maxwell model, as shown in Fig.2(b). Here, k_b is the bracing frame's stiffness and k_d is the damper's stiffness and they are assumed to be constant. C(t) is the damper's damping coefficient. The C(t) of the conventional linear viscous oil damper is constant, but the C(t) of the variable oil damper can be changed from virtually zero ($C_{\min}$) to a very large value ($C_{\max}$) by adjusting the control valve opening. $C_{\min}$ is the damping coefficient when the valve is fully open and $C_{\max}$ is that when the valve is closed. Because of the nature of the hydraulic mechanism, C(t) is positive in all cases. The energy absorption capacity of a conventional linear viscous damper, or a linear Maxwell model, under a harmonic motion $x=\delta \sin\omega t$ is maximized when the damping coefficient C(t) is set to a constant value k/ω. The maximum energy absorbed per cycle is

$$\Delta W = \frac{\pi}{2} k\delta^2 \tag{1}$$

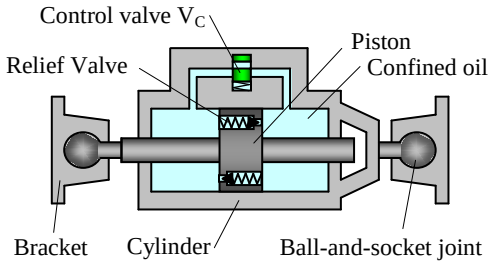

Fig.1 – Basic configuration of variable oil damper

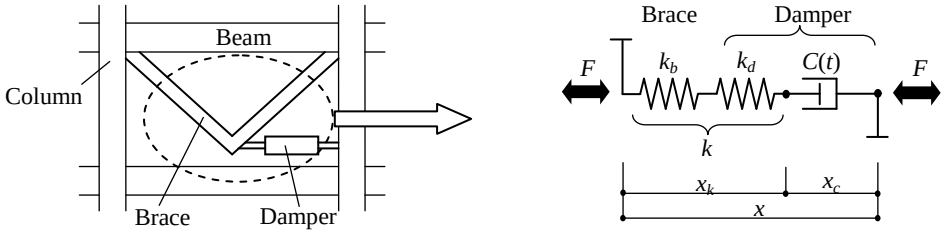

(a) Damper installation (b) Mechanical model

Fig.2 – Mechanical model of a conventional linear viscous oil damper and a variable oil damper

The control algorithm for maximizing the energy absorption of a variable oil damper is expressed by the following on/off or bang-bang control formula [1].

$$\begin{cases} F\dot{x} \geq 0 \ \ or \ \ |F| \leq F_c & : C(t) = C_{\max} \\ F\dot{x} < 0 \ \ and \ |F| > F_c & : C(t) = C_{\min} \end{cases} \tag{2}$$

The first term $F\dot{x}$ expresses the control power of the damper and F_c is a small limit value that the damper can operate.

Fig.3 explains the energy absorption process or the damper's behavior controlled in accordance with Eq. (2). When the damper force and velocity directions are the same, or the control power is positive, $C(t)$ is set to $C_{\max}$ to make the damper as stiff as possible. In this way, the device behaves just like a spring that accumulates the strain energy associated with the spring stiffness and the displacement motion. When the device motion changes direction, or the control power becomes negative, $C(t)$ is switched to $C_{\min}$ in order to quickly dissipate the stored strain energy as heat through viscous dissipation within the damper valve. When the damper force is removed and becomes smaller than F_c, $C(t)$ is switched to $C_{\max}$ again. Fig.3(d) shows the idealized force-displacement relations comparing the variable oil damper with the conventional linear viscous damper under a harmonic motion. The rectangular loop shape of the variable oil damper is kept similar under any frequency or amplitude, and this is the significant feature of the control law of Eq.(2). The energy absorbed per cycle is

$$\Delta W = 4k\delta^2 \tag{3}$$

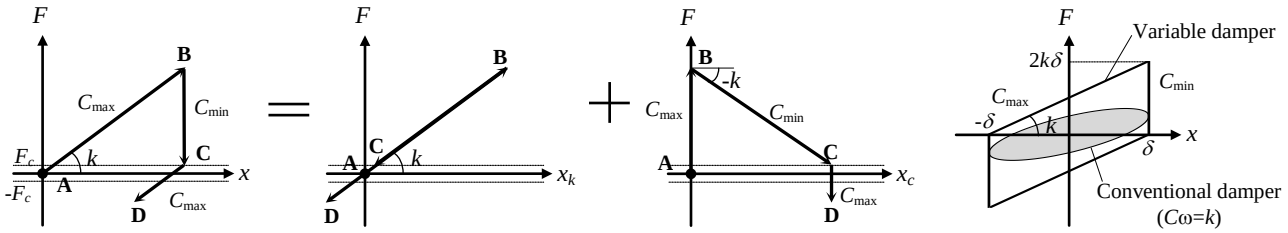

(a) Maxwell model total (b) Spring element (c) Dashpot element (d) Stationary state

Fig.3 – Principle and energy absorption process of variable oil damper

Comparing Eq.(1) with Eq.(3), we can see that the variable oil damper absorbs more than twice the energy as the conventional linear viscous damper. In this paper this variable oil damper is called "variable damper" and the conventional linear viscous damper is called "conventional damper".

3. Concept of energy recovery for oil damper

3.1 Basic configuration of proposed semi-active oil damper with energy recovery system

Here, we propose a semi-active oil damper with an energy recovery system whose basic configuration is shown in Fig.4. This damper has two more control valves and an auxiliary oil tank on the variable oil damper. These additional valves and the tank configure the energy recovery system. Existing oil dampers, including variable types, always change the vibration energy to heat. However, the proposed damper recovers the vibration energy as strain energy of oil in the tank and reuses it at an optimum timing to improve the control efficiency by controlling the opening of the additional valves.

The mechanical model of the proposed damper is expressed as a four-element model shown in Fig.5(b), consisting of a Maxwell model and a Voigt model in series. The spring element of the additional Voigt model, which represents the energy recovery system, plays an important role. Here, F indicates the force of the whole damper, f indicates the force of the tank, k indicates the bracing frame's stiffness including the damper's own stiffness, $C(t)$ is the damping coefficient due to the control valve V_C, k_T is the tank stiffness, $\eta(t)$ is the damping coefficient due to the control valve V_A or V_B, x indicates the story drift, x_k indicates the spring deformation, d indicates dashpot deformation, x_c indicates the dashpot deformation and x_t indicates the tank deformation. We assume that k is constant, and that $C(t)$ and $\eta(t)$ can be changed from virtually zero ($C_{\min}$ and $\eta_{\min}$) to very large values ($C_{\max}$ and $\eta_{\max}$) by adjusting the valve opening. For the proposed damper, the tank stiffness ratio of the tank stiffness k_T to the bracing stiffness k is very important. Therefore, parameter β (= k_T/k) is introduced.

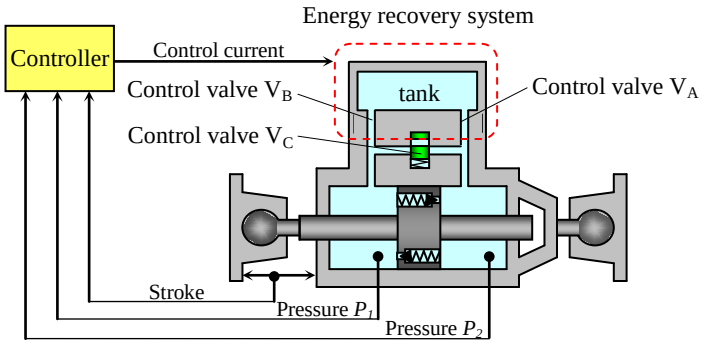

Fig.4 – Basic configuration of proposed semi-active controlled oil damper with energy recovery system

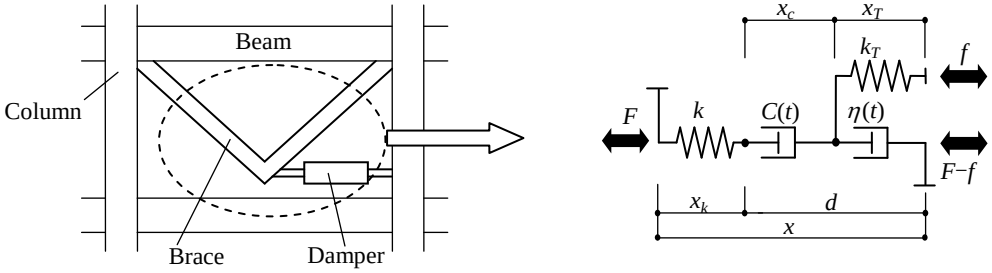

(a) Damper installation (b) Four-element model

Fig.5 – Mechanical model of proposed oil damper

The compatibility condition of the four-element model is expressed by the following simultaneous equations. Here, the first equation of Eq.(4) shows the deformation rate compatibility condition of the whole model and the second shows the deformation rate compatibility condition of the tank. As will be described later, the spring element k_T, which expresses the tank, is a particular element whose force direction changes according to the operation process.

$$\begin{cases} \dfrac{\dot{F}}{k} + \dfrac{F}{C(t)} + \dfrac{F-f}{\eta(t)} = \dot{x} \\ \dfrac{\dot{f}}{k_T} - \dfrac{F-f}{\eta(t)} = 0 \end{cases} \tag{4}$$

3.2 Operation process and energy dissipation capacity of proposed damper

This section describes how to recover and reuse the vibration energy. It is assumed that the variable range of the damper coefficient is sufficiently wide and the sequence of these operations requires only a short time compared to the fundamental vibration period of a building. Fig.6 shows the operation process of the proposed damper installed in the structural frame compared to the frame deformation and the mechanical model. The color expresses the magnitude of pressure: red shows high pressure and pale blue shows low pressure. Fig.7 shows the force-displacement relation, and the variables in Fig.7 are shown in Fig.5(b). All valves are closed under normal conditions and hence the brace is connected rigidly to the frame. The concept of the valve opening when the control power becomes negative is the same as that of the variable damper, but three control valves are operated at that timing sequentially.

[state1→2] All control valves are closed ($C(t)\rightarrow C_{\max}$, $\eta(t)\rightarrow\eta_{\max}$) while control power is positive. Therefore, the spring k deforms and accumulates vibration energy which equals the area of Δ**ABD** in Fig.7(a) as strain energy associated with spring stiffness and displacement motion.

[state2→3] Control valve V_A is opened ($\eta(t)\rightarrow\eta_{\min}$) at **B** in Fig.7(a), when displacement reaches the maximum amplitude. Oil flows from the high-pressure chamber to the tank because the pressure in the tank is lower than that in the high-pressure chamber. The deformation of the spring k_T becomes the same as that of the spring k

associated with this unloading, and the forces of both springs becomes *F'*, which is determined by the balance of both spring stiffnesses. At this time, the spring k_T recovers the strain energy whose amount equals the area of Δ**ACC'** in Fig.7(c). At the same time, the strain energy whose amount equals the area of Δ**ABC** in Fig.7(c) is dissipated through valve V_A. In this way, vibration energy stored in the high pressure chamber is recovered as strain energy of the oil in the tank. It should be noted that, if the force of the spring *k* is F_0 and the force of the spring k_T is f_0 just before the opening of valve V_A, the balanced forces of both springs are expressed by the following equation.

$$F' = f' = \frac{\beta F_0 + f_0}{1+\beta} \tag{6}$$

[state3→4] Control valve V_A is closed ($\eta(t) \rightarrow \eta_{max}$) and control valve V_C is opened ($C(t) \rightarrow C_{min}$) to balance the pressure of both cylinder chambers when the pressures in the high-pressure chamber and tank have balanced. Through this process, the strain energy stored in the spring *k* whose amount equals the area of Δ**CC'D** in Fig.7(c) is dissipated through valve V_C.

[state4→5] Control valve V_C is closed ($C(t) \rightarrow C_{max}$) after the pressures in the chambers are balanced. Then control valve V_B is opened ($\eta(t) \rightarrow \eta_{min}$) and oil flows to the opposite side chamber. In the mechanical model, this

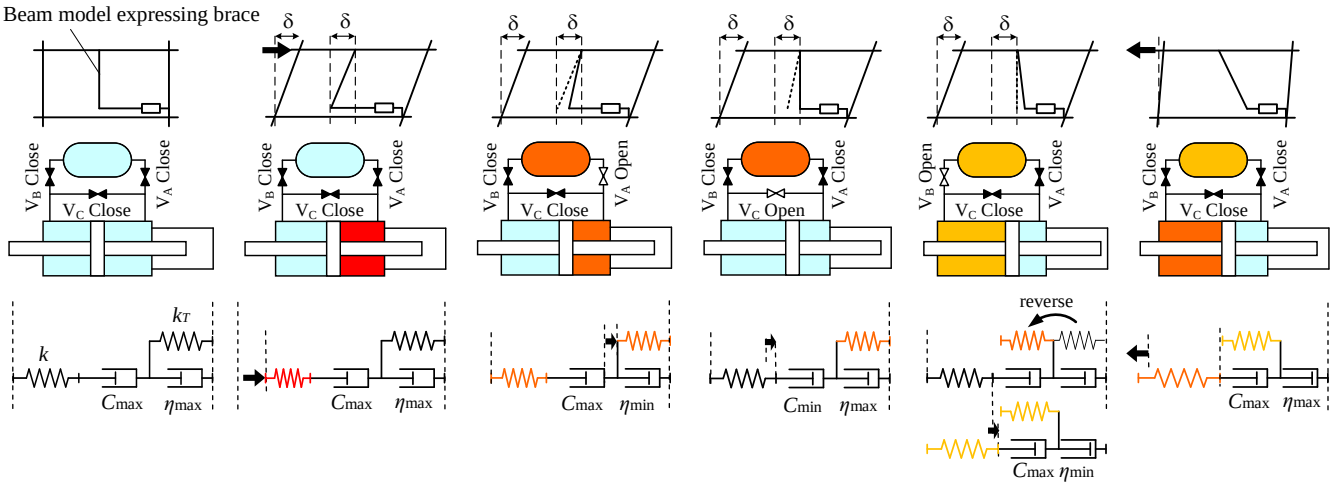

State 1. All valves closed in initial state

State 2. All valves closed until maximum vibration amplitude

State 3. Open V_A and vibration energy stored in tank

State 4. Open V_C and pressure in cylinder balanced

State 5. Open V_B and energy reused to enhance damper stroke

State 6. All valves closed and prepare for reverse direction vibration

Fig.6 – Principle and process of energy recovery system

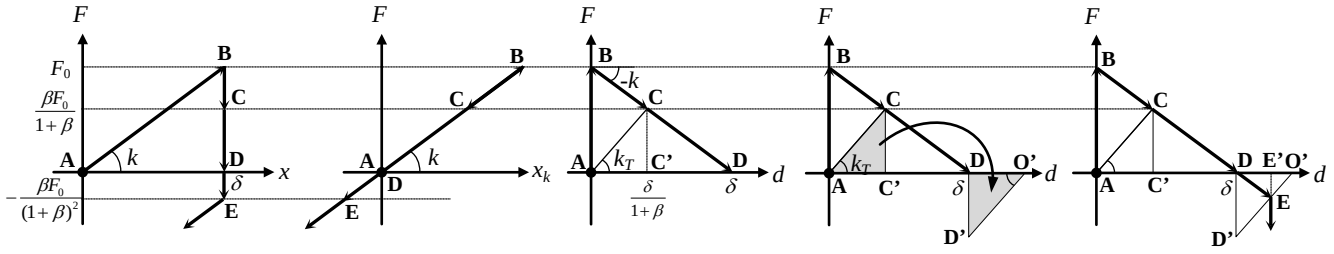

(a) story drift *x*

(b) deformation of *k*

(c) damper deformation State 1-4

(d) damper deformation State 5

(e) damper deformation State 5-6

Fig.7 – Force-displacement relationship of proposed damper

operation is equivalent to reversing the force direction of the spring k_T while maintaining the deformation, and then $\eta(t)$ is switched to $\eta_{\min}$. These operations are equivalent to Δ**ACC'** moved to Δ**O'D'D** being symmetric with respect to a point as shown in Fig.7(d) and Fig.7(e) and then the strain energy of the spring k_T is dissipated through valve V_B. By this operation, a part of the energy stored in the spring k_T, whose amount equals the area of Δ**DEE'** in Fig.7(d), is reused to extend the deformation of the spring k. Therefore the deformation of the spring k that reaches point **E** in Fig.7(e) exceeds the story drift. In this process, the strain energy whose amount equals the area of Δ**DD'E** is dissipated by valve V_B and the strain energy whose amount equals the area of Δ**O'EE'** remains in the tank.

[state5→6] Control valve V_B ($\eta(t)\rightarrow\eta_{\max}$) is closed to prepare for the next vibration (state 6) when the pressures in the tank and high pressure chamber are balanced.

The spring k_T, which represents the tank, gradually accumulates strain energy along with the cyclic loading as described above and its strain energy saturates within several cycles as shown in Fig.8(a). It is clearly observed that the damper force increases with repetition of vibration. If the forces of spring k and spring k_T at point **P** in Fig.8(a) are assumed to be F_0 and f_0, respectively, the forces of these springs at point **Q** in Fig.8(a) are expressed by the following equation.

$$F' = f' = \frac{\beta F_0 + f_0}{(1+\beta)^2} \tag{4}$$

The forces at points **P** and **Q** can be evaluated to equate f' and f_0 and to consider the relation that is $F_0=f_0+2k\delta$. Therefore, the stationary energy absorption capacity is expressed by the following equation.

$$\Delta W = 4\left(\frac{3+\beta}{1+\beta}\right)k\delta^2 \tag{5}$$

Fig.8(b) compares the energy absorption capacity of the proposed damper with those of the conventional damper and the variable damper. Fig.8(c) shows the relationship of the energy absorption capacity and the tank stiffness ratio. If we can set the tank stiffness ratio around 1.0, the energy absorption capacity of the proposed damper is twice that of the variable damper and 4 times that of the conventional damper. Since the bracing frame's stiffness is generally comparable to the device stiffness, setting the tank stiffness ratio around 1.0 means the tank stiffness is set to about half of the device stiffness. This setting can be realized using the tank whose size is comparable to the cylinder. It should be noted that this rectangular loop shape of the proposed damper inherently associated with the switching control law is kept similar under any frequency or amplitude, as for the variable damper.

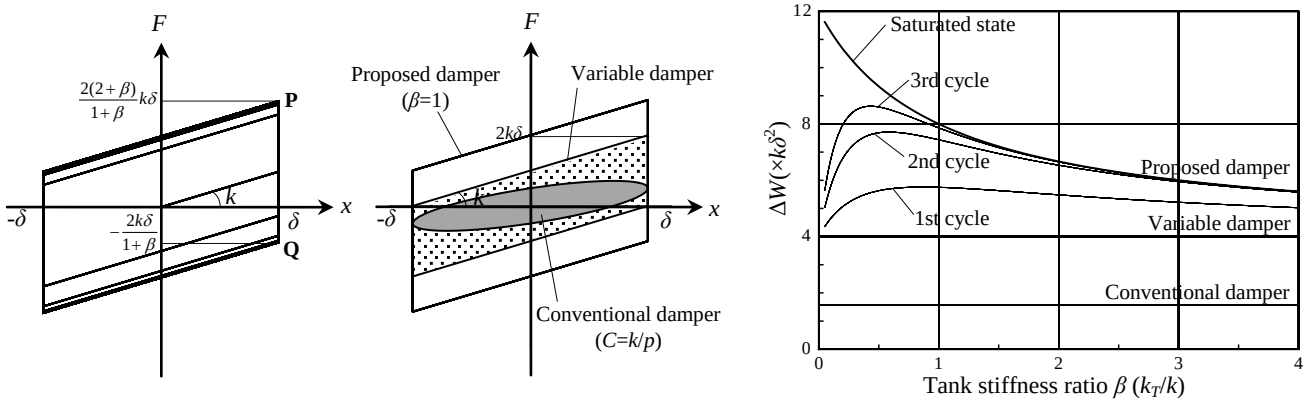

(a) Cyclic behavior (b) Stationary state (c) $\Delta W - \beta$ relationship

Fig.8 – Energy absorption capacity of proposed damper

4. Dynamic loading test on full-scale specimen and simulation analyses

4.1 Specimen overview and hydraulic circuit involving energy recovery system

Fig.9 shows an external view of the full-scale specimen and Table 1 shows its specifications. All the components of the hydraulic circuit, except the main relief valves, are housed in the valve block, and the valve block and the auxiliary tank are attached to the cylinder. The main relief valves that limit the force generated under unexpected large motions to protect the device from overload are built into the piston. The major parts that contribute to generation of a large reaction force, such as cylinder and piston, are the same as those of previously developed conventional dampers, and there is a ball-and-socket joint at each end. The capacity of the tank, which is the key

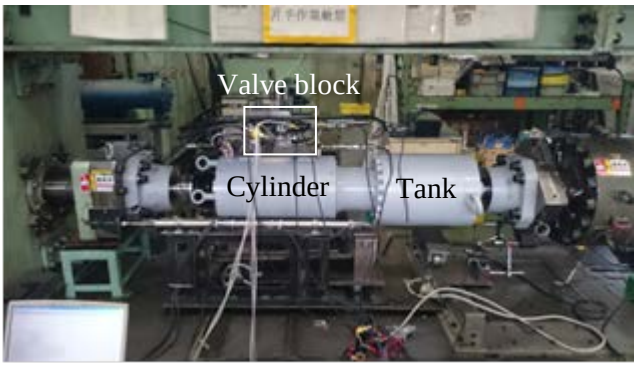

Fig.9 – External view of full-scale proposed damper

Table 1 Specifications of full-scale proposed damper

Maximum design force	2100kN
Relief force	1500kN
Maximum pistion stroke	±80mm
Size	φ365mm, 1.92m
Stiffness k_d	405kN/mm

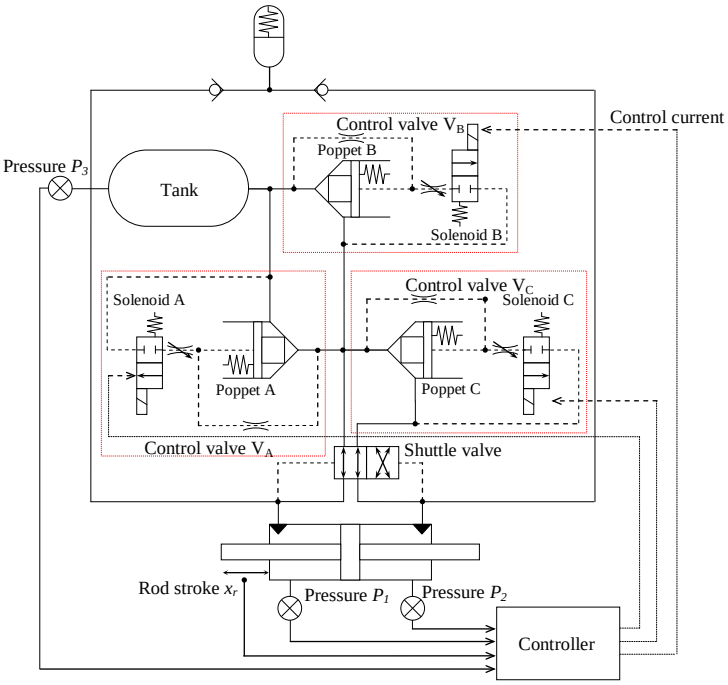

Fig.10 – Hydraulic circuit

component of the energy recovery system, is determined by setting the target stiffness k_T to about half the device stiffness k_d. This setting can set the tank stiffness ratio β to 1.0 when the stiffness of the connected braces is same as the device stiffness k_d.

Fig.10 shows a hydraulic circuit involving the energy recovery system. The relief valve is omitted from Fig.10 for convenience. Each control valve consists of a poppet valve and a solenoid. Normally, the solenoid and the poppet valve are closed. When the control current is provided to the solenoid, the solenoid opens first, and then the poppet valve opens corresponding to the solenoid by pressure control. Since the hydraulic circuit uses a shuttle valve, the order in which the valve opens is always the same regardless of the movement direction of the piston. The controller provides the current to each solenoid at the timing described in section 2.3 according to the signal processing flow using the signals of the pressure sensors and stroke sensor. This device can operate as a variable damper to control only control valve V_C if V_A and V_B are closed compulsively.

It is also a major feature to adopt the decentralized control system developed for the semi-active variable damper [1]. Large-scale wiring throughout the building is not necessary because the controller needs only sensor signals provided from built-in sensors.

4.2 Experimental method

In order to evaluate the logical motion of the developed valve system and the energy absorption capacity, as well as its durability, we conducted dynamic loading tests on a full-scale damper designed for actual application. The loading setup is shown in Fig.11(a). A dynamic actuator is used for this test. Fig.11(b) shows a mechanical model and characteristics of the experimental setup, and this is equivalent to the model in Fig.5(b) if k_b is assumed as the loading frame stiffness. The loading frame stiffness was evaluated as about 700kN/mm by the experiment conducted beforehand. Whole stiffness k involving the frame stiffness is about 250kN/mm and the tank stiffness is 200kN/mm. Therefore, the tank stiffness ratio β is 0.8. The actuator displacement is equivalent to the displacement between stories in an actual building, and we operate the actuator using a signal equivalent to this displacement.

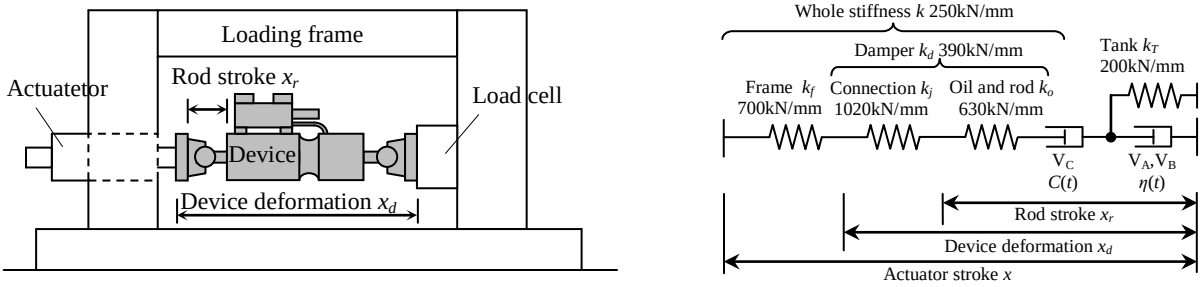

(a) Experimental setup (b) Mechanical model

Fig.11 –Experimental setup and mechanical model

4.3 Experimental results and simulation analyses

First, we conducted sinusoidal loading tests in which amplitude of the actuator stroke x was increased to 3mm by in 1mm steps every 3 cycles. Fig.12 shows a part of the time histories of the device force F and the tank force f. When V_A or V_B are opened, the device force and the tank force balance at the point evaluated from mechanical consideration using a four-element model. This proves that the behavior of this device agrees with the theoretical prediction.

Force-device deformation relations obtained under sinusoidal loading for 0.2, 0.3 and 0.5Hz are shown in Fig.13, Fig.14 and Fig.15. Fig.13 shows the results when all valves are closed compulsively for reference. Under this condition, the device behaved like a spring and these results show that the maximum damping coefficients $C_{\max}$ and $\eta_{\max}$ are very large. These maximum damping coefficients evaluated by these test results are about 3000kNs/mm. Fig.14 shows the results for the variable damper. It is recognized that it realizes a characteristic rectangular loop. Fig.15 shows the results for the proposed damper. The characteristic rectangular loops associated with the control law and energy recovery system were accurately realized here, which means that the

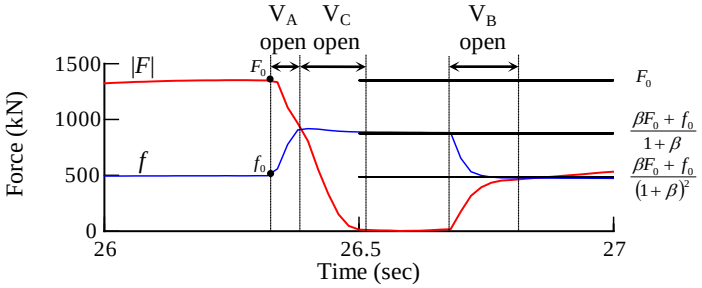

Fig.12 –Force time histories of proposed damper under sinusoidal loading 0.2Hz

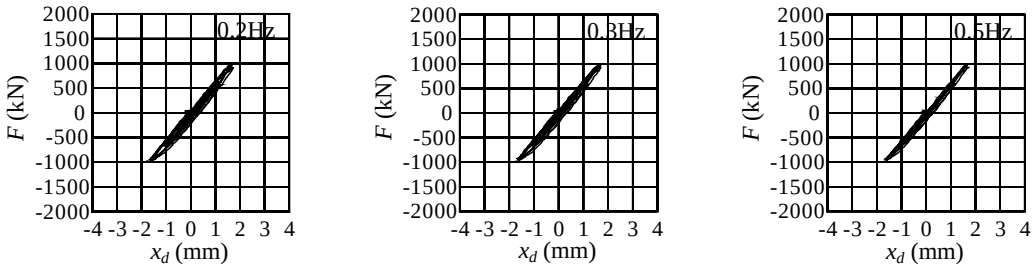

Fig.13 –Force-displacement relation for sinusoidal loading (All valves closed)

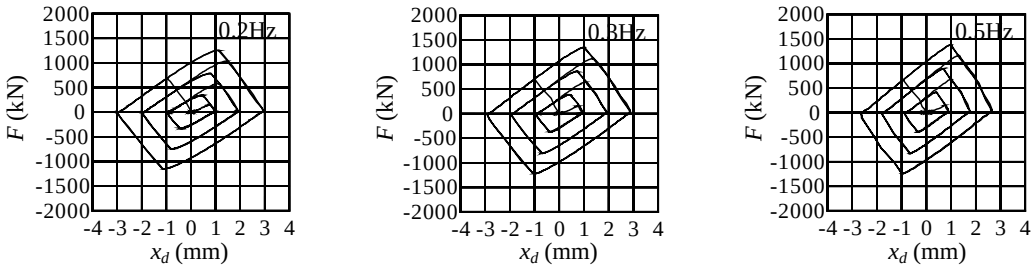

Fig.14 –Force-displacement relation of variable damper for sinusoidal loading (V_C controlled)

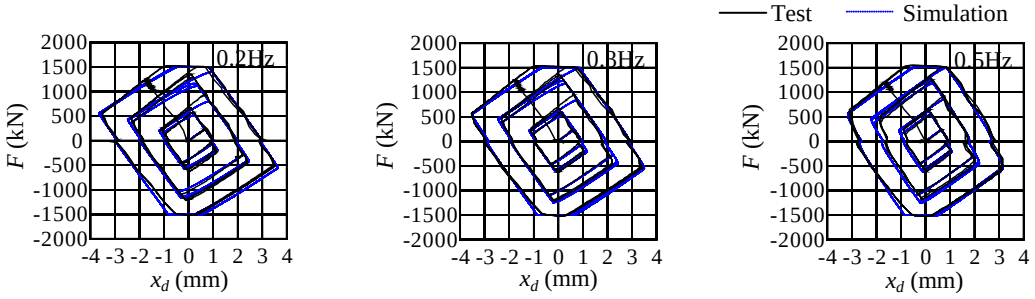

Fig.15 –Force-displacement relation of proposed damper for sinusoidal loading (All valves controlled)

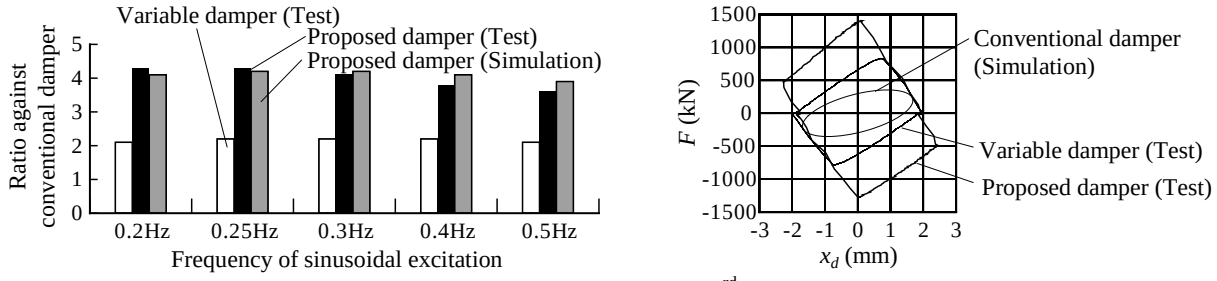

(a) Energy absorption capacity ratio (b) 3rd loop of each dampers with 2mm amplitude (0.2Hz)

Fig.16 –Energy absorption capacity ratio against conventional damper

expected valve operation was adequately realized by semi-active control. The rectangular loop shapes of these results are kept similar under any frequency or amplitude as theoretically expected. When the device force becomes zero, the damper deformation is the same as the actuator stroke. After that, the damper deformation exceeded the actuator stroke because of the energy recovery system. Therefore, the energy absorption capacity is significantly improved. Fig.16 shows the energy absorption capacity ratio against a conventional damper. The energy absorption capacities are evaluated from the 3rd loop whose amplitude is 2mm for each damper. The energy absorption capacity of the proposed damper is twice that of the variable damper and approximately 4 times that of the conventional damper as theoretically expected in section 3.2.

To examine the dynamic behavior under non-stationary excitation, a dynamic loading test was conducted using a seismic response wave of a 30-story building model for design earthquake in Japanese code. Fig.17 shows the time histories of loading displacement, generated damping force, absorbed energy, and the force-displacement relation. It is confirmed that the valves operate stably based on the semi-active control even under such a non-stationary loading condition. A simulation result using a four-element model, which simply changes the damping coefficient corresponding to the operation process shown in section 3.2, is also shown in the figure. It is confirmed that the dynamic behavior of the device can be accurately simulated by a proposed analytical model.

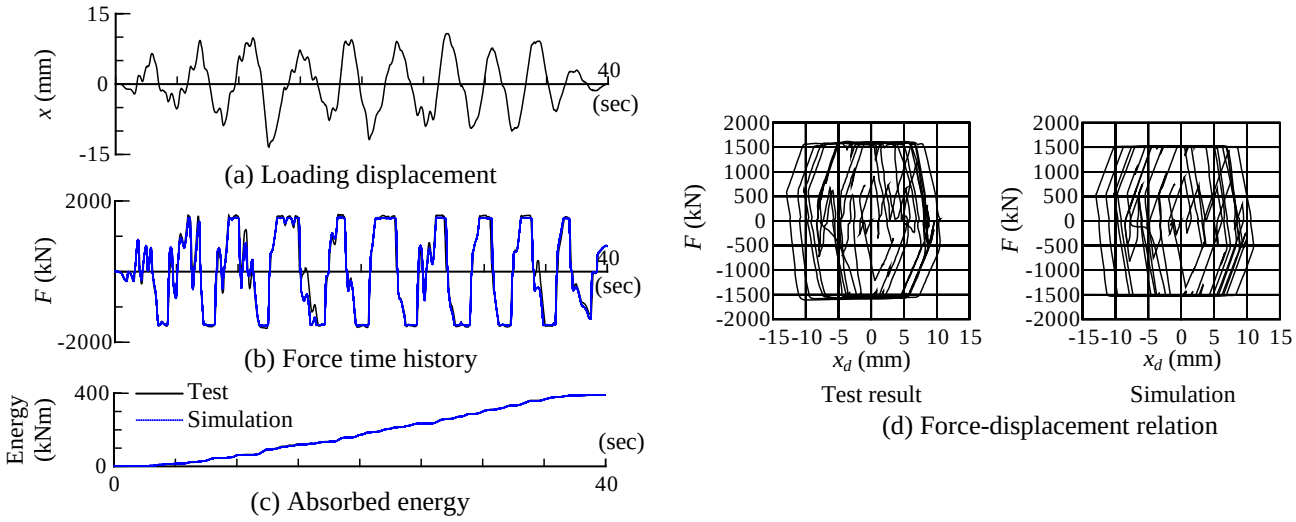

Fig.17 – Test results and simulations for structural seismic response waves

5. Seismic response analyses of a high-rise building model

5.1 High-rise building model and analytical condition

In order to evaluate the effectiveness of the proposed damper, we conducted a seismic response analysis using a 35-story building model. The total weight of the building is 1600MN, and Fig.18(a) shows the representative framing elevation. We assume that total 54 dampers are installed from the 1st to 6th stories, and only one direction is considered in this study. The building is modeled by a 3-dimensional frame model. The first mode's natural period is 4.68 seconds, and an initial structural damping ratio of 1.0% is assumed for the first mode. All members of this model are assumed to be elastic. We consider four damper conditions,

Case 1 : Open frame (without damper)
Case 2 : Conventional damper
Case 3 : Variable damper
Case 4 : Proposed damper with energy recovery system

The damping coefficient of the conventional damper is set to 80kNs/mm to maximize the additional damping to the structure based on the resonant curve. The parameters of the variable damper and the proposed damper are determined by test results. Force limitation by a relief valve is also considered here (1700kN per

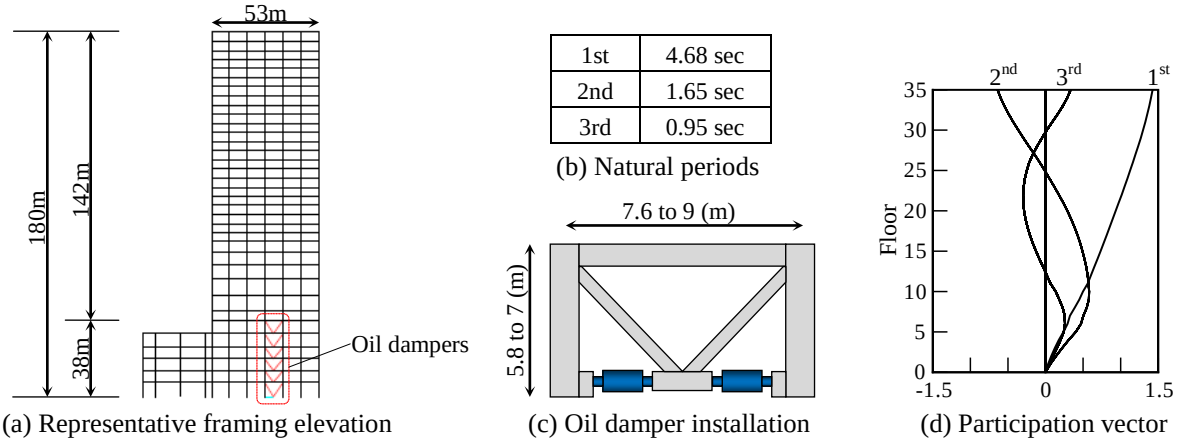

(a) Representative framing elevation (b) Natural periods (c) Oil damper installation (d) Participation vector

Fig.18 – Building model for seismic response analysis

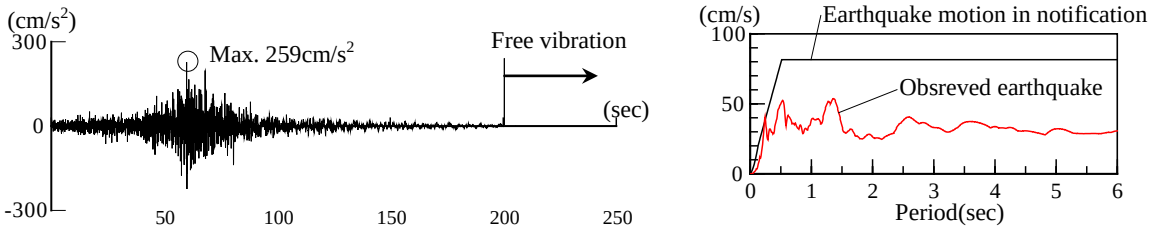

(a) Acceleration time history (b) Velocity response spectrum (h=5%)

Fig.19 – Input earthquake

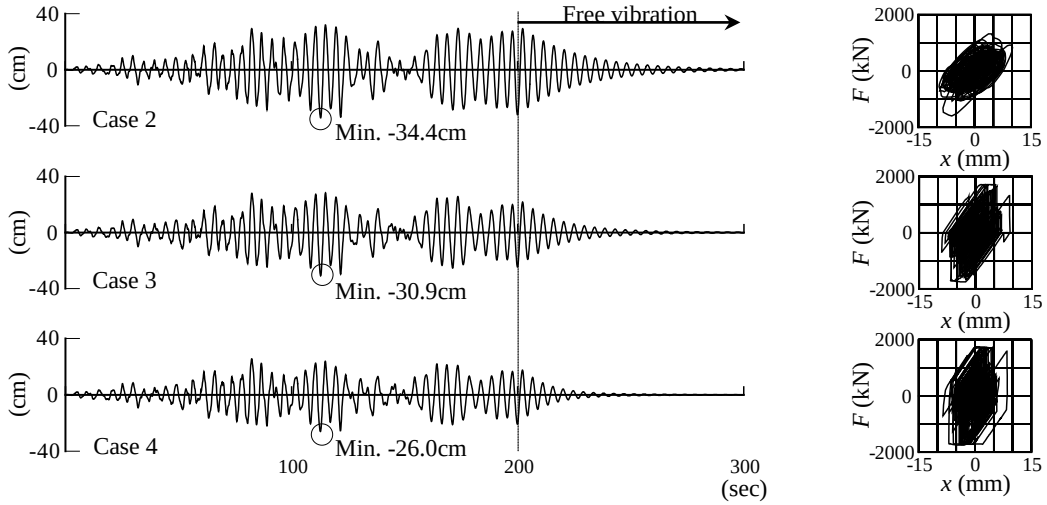

Fig.20 – Response displacement time histories and force-displacement relations

device). The ground acceleration observed in Tokyo in the Great East Japan Earthquake of 2011 is used for the input excitation. Fig.19 shows the acceleration time history and the response spectrum of the input ground motion compared with the earthquake in Japanese code. After 200 seconds, the input ground motion is set to zero to evaluate the convergence time of vibration.

4.2 Analytical result

Fig.20 shows the response displacement time histories of the roof floor and the relations between the damper force and the story drift in the 2nd story for cases 2 to 4. After 200 seconds, we can see the free vibration waves.

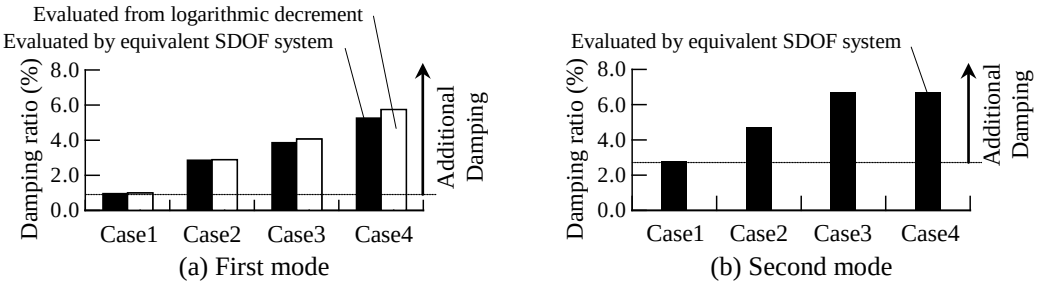

Fig.21 – Damping ratio

It is observed that the response displacement of the proposed damper case is kept small during the earthquake and the convergence time of vibration is obviously shorter than that of other cases.

Fig.21 shows the damping ratio estimated by the following method. First, the displacement time histories until 200 seconds are decomposed to modal responses using the participation vector. Next, a Single Degree of Freedom (SDOF) system that makes the mean-square error the smallest is identified. As a result, the natural period and the damping ratio of the SDOF system are identified as those of each mode. These results are shown as black bars in Fig.21. The white bars in Fig.21(a) are the results evaluated from logarithmic decrement of the free vibration waveform after 200 seconds. It is observed that the additional damping ratio to the first mode of the proposed damper is larger than approximately 2.3 times that of the conventional damper and approximately 1.5 times that of the variable damper. These promising results confirm the feasibility and effectiveness of the proposed damper under actual application conditions.

6. Conclusions

We have presented a novel semi-active oil damper developed to break through the limitations of existing oil dampers by introducing a unique energy recovery system. This device can dissipate 4 times as much energy as a conventional linear viscous damper and twice as much as a variable oil damper based on the on/off algorithm by using vibration energy to enhance the damper stroke with flow control valves and an auxiliary oil tank. One remarkable feature of this system is that the control loop is closed in each device, and each device is equipped with all of the control equipment. To investigate the proposed energy recovery system's effectiveness and the damper behavior, dynamic loading tests were conducted on a full-scale device. This device showed stable performance even under a nonstationary loading as well as under a sinusoidal loading, and highly improved energy absorption capacity was recognized. It is also confirmed that the damper's dynamic behavior can be accurately simulated using a four-element model and the results of seismic response analyses using a high-rise building model equipped with the propose damper showed higher control effect than other oil dampers.

7. Acknowledgements

The authors wish to express their appreciation to Dr. Qian of Senqcia Co., Ltd. for his contribution to production of the actual system.

8. References

[1] Kurino H, Tagami J, Shimizu K, Kobori T (2003): Switching oil damper with built-in controller for structural control. *Journal of Structural Engineering*, ASCE, **Vol.129 No.7**, 895-904.

[2] Kurino H, Orui S, Shimizu K (2010): Control Effect of Semi-active On/Off Oil Damper Installed in Actual High-rise Building for Large Earthquake and Strong Winds. *5th World Conference on Structural Control and Monitoring*, Tokyo, Japan.

[3] Kurino H, Matsunaga Y, Yamada T, Tagami J (2004): High performance passive hydraulic damper with semi-active characteristics. *13th World Conference on Earthquake Engineering*, Vancouver, Canada.